EPJ Web of Conferences **29**, 00025 (2012)
DOI: 10.1051/epjconf/20122900025

Effect of Gaussian doping profile on the performance of a thin film polycrystalline solar cell

S. Kolsi[1,a], M. Ben Amar[2], H. Samet[3], and A. Ouali [1]

[1]Research Unit Advanced and Control and Energy Management, ACEM, Department of Electrical Engineering, Sfax National Engineering School, University of Sfax, BP. 1173, 3038, Sfax, Tunisia.
[2]Department of Physics, Science Faculty of Sfax, University of Sfax, BP. 1171, 3000, Sfax, Tunisia.
[3]Electronic Laboratory and Information Technology, LETI, Department of Electrical Engineering, Sfax National Engineering School, University of Sfax, BP. 1173, 3038, Sfax, Tunisia.

Abstract. A two-dimensional (2D) analytical model based on the Green's Function method is applied to an n^+-p thin film polycrystalline solar cell that allows us to calculate the conversion efficiency. This model considers the effective Gaussian doping profile in the p region in order to improve cell efficiency. The dependence of mobility and lifetime on grain doping is also investigated. This model is implemented through a simulation program in order to optimize conversion efficiency while varying thickness and doping profile in the base region of the cell. Compared with n^+-p standard structure, our proposed structure shows a 43% improvement in conversion efficiency for a polycrystalline solar cell.
PACS. 85.30.De Semiconductor-device, characterization, design and modelling.
88.40.hj Efficiency and performance of solar cells.

Nomenclature

I_{ph} : total photo generated current(A).
I_{sd}: saturation diffusion dark current (A).
I_{sr} : saturation recombination dark current (A).
I_{sc} : short circuit current (A).
V_{oc}: open circuit voltage (V).
R_s: series resistance (Ω).
R_{sh} : shunt resistance (Ω).
I: output current (A).
V: voltage delivered by the cell (V).
I_m : current at maximum power point (A).
V_m : voltage at maximum power point (V).
q : electron charge (1,6 10^{-19} C).
T: cell temperature (K).
V_T: thermal voltage (V).
P_i : incidence irradiance under AM1 illumination condition on the PV cell surface (W/m^2).
N_d: concentration doping density of emitter (cm^{-3}).
H: thickness of semiconductor (µm).
d: grain width (µm).
K: Boltzmann's constant (J/K).
n_i : Silicon intrinsic carrier concentration (cm^{-3}).
ε_o : emptiness permittivity ($F.cm^{-1}$).
ε_r : relative silicon permittivity.
α_i : absorption coefficient related to the incident wavelength λ_i (μm^{-1}).
$g_{i,0}$: the silicon generation rate related to the incident wavelength λ_i ($cm^{-3}s^{-1}$).
D_n: diffusion constant of electrons (cm^2/s).
D_p: diffusion constant of holes (cm^2/s).
L_n: diffusion length of electrons (cm).
L_p: minority carrier diffusion length in the emitter region (cm).

[a] e-mail : sami_kolsi@yahoo.fr

W_e: emitter thickness (µm).
W: space charge region width (µm).
μ_p: mobility of holes (cm^2.V/s).
S_P: recombination velocity at the frontal surface (cm/s).
μ_n: mobility of electrons (cm^2.V/s).
W_b: base layer thickness (µm).
S_n: recombination velocity at rear contact (cm/s).
I_{ph} : total photo generated current(A).
I_{sd}: saturation diffusion dark current (A).
N_{a2}: doping density at the limit of rear contact (cm^{-3}).
N_{a1}: doping density in p region at the space charge layer limit (cm^{-3}).
V_g: effective recombination velocity at the grain boundary in base and emitter region (cm/s).
A: the cell area (m^2).
τ_n: electrons lifetime (s).
τ_p: holes lifetime (s).
N_d: concentration doping density of emitter (cm^{-3}).
H: thickness of semiconductor (µm).

1 Introduction

The important factor in photovoltaic production is cell cost. One of the promising ways of reducing this cost is by reducing direct material cost. So polycrystalline silicon is actually the most convenient and most used material for solar cells because of its low production cost as well as its reasonable conversion efficiency [1,2]. Several techniques have been used to increase the efficiency of polysilicon solar cells. Some techniques are meant to reduce recombination at grain boundary by the process of preferential doping [3], others use bulk and surface passivation [4] with ionic implantation or thermal diffusion [5,6]. Other techniques are used to reduce the effect of back surface recombination velocity by means of the Back Surface Field technique (BSF) [7]. These techniques have to be used to improve the collection of photo generated carriers at the depletion edge so as to increase the conversion efficiency of the cell.

In this work, we propose a new technique to reduce the minority carriers' recombination at rear contact and improve the open circuit voltage. We develop a two-dimensional analytical model which enables us to calculate the photocurrent and the dark current in each region of the n^+-p structure in the case of Gaussian doping profile in p region. We use a two-diode electrical model in order to determine the conversion efficiency of the considered cell. We compare the performance of the considered cell with standard structure.

2 Theory development

2.1 Physical model of an elementary solar cell

The structure of the thin film Polycrystalline solar cell presented in Fig. 1 is divided into three main regions: (emitter (n^+), space charge region (n^+-p) and base region (p)). According to this model, the thickness of these regions is W_e, W and W_b respectively.
The following considerations have been introduced in order to simplify our model:
(i) The grains are considered as columnar and perpendicular to the n^+-p junction [9], and their electrical properties are homogeneous (doping concentration, minority carrier mobility, lifetime and diffusion length).
(ii) The minority carrier mobility and lifetime in base and emitter regions depends only on the doping level for the corresponding region.
(iii) Grain boundary recombination is negligible in the heavily doped emitter [9] and in the space charge region [10]. This is in agreement with Green [11].
(iv) We assume that low-level injection conditions prevail.

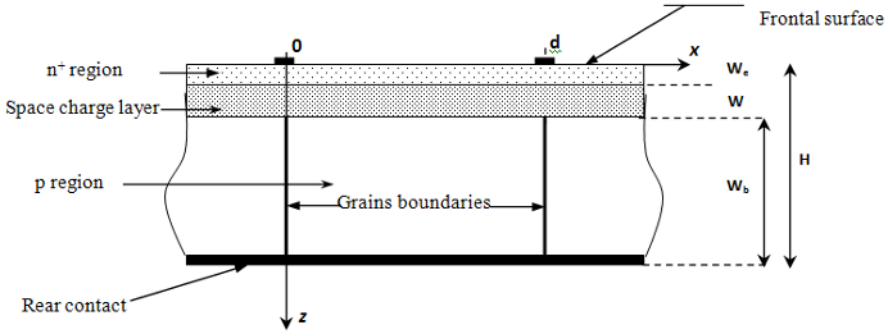

Fig. 1. Schematic model of the polycrystalline solar cell

2.2 Photo generated current

The minority carrier density Δn generated in the base region can be obtained by solving the two-dimensional continuity equation for the electron given by:

$$\frac{\partial^2 \Delta n}{\partial z^2}+\frac{\partial^2 \Delta n}{\partial x^2}+\frac{\Delta n}{V_T}\frac{\partial E}{\partial z}+\frac{E}{V_T}\frac{\partial \Delta n}{\partial z}-\frac{\Delta n}{L_n^2}=-\frac{g_i(z)}{D_n} \tag{1}$$

Where:

$g_i(z)=g_{i,0}\exp(-\alpha_i z)$ and $V_T=\frac{KT}{q}$

The Gaussian doping profile in the base region is considered. $N_a(z)$ is given by :

$$N_a(z)=N_{a2}\exp\left(-\left(\frac{z-H}{\delta}\right)^2\right) \tag{2}$$

δ is the characteristic coefficient of the Gaussian function given by:

$$\delta=\frac{W_b}{\sqrt{\ln(N_{a2}/N_{a1})}} \tag{3}$$

In this condition, there is an impurity concentration gradient that induces an electric field E in the base region given by:

$$E(z)=\frac{V_T}{N_a(z)}\frac{dN_a(z)}{dz} \tag{4}$$

We note that L_n, D_n and E depend on the doping density which depends on the distance z. Consequently, equation (1) is in the second order differential equation that is not easy to solve when the coefficients depend on z. To simplify our study, we consider the average value of N_a, D_n, L_n and E given by:

$$\overline{N_a}=\frac{1}{W_b}\int_{H-W_b}^{H}N_a(z)dz \tag{5}$$

$$\overline{L_n}=\sqrt{\overline{\tau_n}\,\overline{D_n}} \tag{6}$$

$$\overline{D_n}=\overline{\mu_n}V_T \tag{7}$$

$$\overline{E} = \frac{1}{W_b}\int_{H-W_b}^{H} E(z)dz \tag{8}$$

Where $\overline{\mu_n}$ and $\overline{\tau_n}$ are respectively the electrons mobility and lifetime given by [12-13]:

$$\overline{\mu_n} = 232 + \frac{1180}{1+\left(\frac{\overline{N_a}}{8\times10^{16}}\right)^{0,9}} \tag{9}$$

$$\overline{\tau_n} = \left(3{,}54\times10^{-12}\overline{N_a} + 0{,}95\times10^{-31}\overline{N_a}^2\right)^{-1} \tag{10}$$

Under these conditions equation (1) can be rewritten as:

$$\frac{\partial^2\Delta n}{\partial z^2} + \frac{\partial^2\Delta n}{\partial x^2} + \frac{\overline{E}}{V_T}\frac{\partial\Delta n}{\partial z} - \frac{\Delta n}{\overline{L_n}^2} = -\frac{g_i(z)}{\overline{D_n}} \tag{11}$$

Equation (12) is subjected to the following boundary conditions when the device is operated under short circuit:

$$\Delta n(x, z = H - W_b) = 0 \tag{12}$$

$$\left.\frac{\partial\Delta n}{\partial x}\right|_{z=H} + \frac{\overline{E}}{V_T}\Delta n(x, z = H) = \frac{-S_n}{\overline{D_n}}\Delta n(x, z = H) \tag{13}$$

$$\left.\frac{\partial\Delta n}{\partial x}\right|_{x=0} = \frac{V_g}{2\overline{D_n}}\Delta n(x = 0, z) \tag{14}$$

$$\left.\frac{\partial\Delta n}{\partial x}\right|_{x=d} = \frac{-V_g}{2\overline{D_n}}\Delta n(x = d, z) \tag{15}$$

In order to calculate the total minority carrier density generated in the base region using AM1 illumination condition, we consider the assumption proposed by Mohammed et al. [14] which decomposes the solar spectrum into four wavelengths. The absorption coefficient and generation rate in AM1 illumination condition α_i (μm^{-1}) and $g_{i,0}$ ($cm^{-3}s^{-1}$) are listed in Table 1 [15].

Table 1. Absorption coefficient α_i, generation rate $g_{i,0}$ related to the incident wavelength λ_i under AM1 illumination condition (P_i=925 W/m^2).

α_i (μm^{-1})	$6{,}33079\times10^{-2}$	$1{,}02664\times10^{-2}$	7×10^{-4}	1,76058
$g_{i,0}$ ($cm^{-3}s^{-1}$)	$6{,}46746\times10^{19}$	$5{,}54674\times10^{18}$	$9{,}26415\times10^{17}$	$2{,}03553\times10^{21}$

Using the Green function [16,17], the excess minority carrier density of electron is given by:

$$\Delta n(x, z) = \sum_{i=1}^{4}\sum_{k=1}^{\infty} f_{k,i}(z) M_k \cos\left(C_k\left(x - d/2\right)\right) \tag{16}$$

The C_k coefficients are obtained by the following transcendental equation [9,16]:

$$tg\left(\frac{C_k d}{2}\right)=\frac{V_g}{2C_k\overline{\overline{D_n}}} \tag{17}$$

The general solution of $f_{k,i}$ is given by:

$$f_{k,i}(z)=\frac{g_{i,0}}{\overline{\overline{D_n}}\left(\mu_k^2+2\alpha_i\beta-\alpha_i^2\right)}\left\{e^{-\alpha_i z}-\frac{e^{\beta(H-z)}e^{-\alpha_i H}\left[e^{\alpha_i W_b}\left(v_k ch\left(v_k(H-z)\right)+(\gamma-\beta)sh\left(v_k(H-z)\right)\right)-(\gamma-\alpha_i)e^{\beta W_b}sh\left(v_k(H-Wb-z)\right)\right]}{e^{\beta W_b}\left[v_k ch\left(v_k W_b\right)+(\gamma-\beta)sh\left(v_k W_b\right)\right]}\right\} \tag{18}$$

where:

$$\beta=\frac{\overline{E}}{2V_T};\ \mu_k=\left(C_k^2+\frac{1}{\overline{\overline{L_n^2}}}\right)^{1/2};\ \gamma=\frac{\overline{E}}{V_T}+\frac{S_n}{\overline{\overline{D_n}}};\ v_k=\left(\beta^2+\mu_k^2\right)^{1/2};\ M_k=\frac{4\sin\left(C_k d/2\right)}{C_k d+\sin\left(C_k d\right)}$$

The carrier density in the base region is calculated for k varying from 1 to 10, which has been found to be sufficient to obtain a good convergence whatever the grain dimensions and the superficial recombination velocities.

$$J_b=\frac{q\overline{\mu_n}\,\overline{E}}{d}\int_0^d \Delta n(x,z)\big|_{z=H-W_b}dx+\frac{q\overline{D_n}}{d}\int_0^d \left.\frac{\partial\Delta n(x,z)}{\partial z}\right|_{z=H-W_b}dx \tag{19}$$

In the emitter region, we consider the uniform doping level. Using the same method, the current density J_e generated in the emitter region can be written as:

$$J_e=\sum_{i=1}^{4}\sum_{j=1}^{\infty}\left[\frac{-8qg_{i,0}\sin\left(\frac{C_j d}{2}\right)L_j}{dC_j\left(C_j d+\sin(C_j d)\right)\left(\alpha_i^2L_j^2-1\right)}\times B_{i,j}\right] \tag{20}$$

$B_{i,j}$ is given by:

$$B_{i,j}=\frac{\left(\frac{D_p\alpha_i}{S_p}+1\right)+e^{-\alpha_i W_e}\left[ch\left(\frac{W_e}{L_j}\right)+\frac{D_p}{L_j S_p}sh\left(\frac{W_e}{L_j}\right)\right]}{sh\left(\frac{W_e}{L_j}\right)+\frac{D_p}{L_j S_p}ch\left(\frac{W_e}{L_j}\right)}-L_j\alpha_i e^{-\alpha_i W_e} \tag{21}$$

The L_j coefficients are defined by:

$$L_j^2=\left(C_j^2+L_p^{-2}\right)^{-1} \tag{22}$$

L_p is given by:

$$L_p=\sqrt{\mu_p\tau_p V_T} \tag{23}$$

μ_p and τ_p are defined as [18]:

$$\mu_p = 130 + \frac{370}{1 + \left(\frac{N_d}{8 \times 10^{17}} \right)^{1,25}} \tag{24}$$

$$\tau_p = \left(7,8 \times 10^{-13} N_d + 1,8 \times 10^{-31} N_d^2 \right)^{-1} \tag{25}$$

The C_j coefficients are obtained by the following transcendental equation:

$$tg\left(\frac{C_j d}{2} \right) = \frac{V_g}{2 C_j D_p} \tag{26}$$

where V_g is the recombination velocity at x=0 and x=d.
The contribution of the space charge region is given as follows [19]:

$$J_{scr} = \sum_{i=1}^{4} \frac{q g_{i,0} \exp\left(-\alpha_i W_e\right)}{\alpha_i} \left[1 - \exp\left(-\alpha_i W\right) \right] \tag{27}$$

where W is given by [19]:

$$W = \left[\frac{2 \varepsilon K T}{q^2 \overline{N_a}} \ln\left(\frac{\overline{N_a} N_d}{n_i^2} \right) \right]^{\frac{1}{2}} \tag{28}$$

The total photocurrent density generated by the cell is given by:

$$J_{ph} = J_e + J_b + J_{scr} \tag{29}$$

2.3 Dark current

In order to calculate the dark current in the base region, we solve the continuity equation given by:

$$\frac{\partial^2 \Delta n_0}{\partial z^2} + \frac{\partial^2 \Delta n_0}{\partial x^2} + \frac{\overline{E}}{V_T} \frac{\partial \Delta n_0}{\partial z} - \frac{\Delta n_0}{\overline{L_n}^2} = 0 \tag{30}$$

with the general solution:

$$\Delta n_0(x, z) = \sum_{k=1}^{\infty} g_k(z) M_k \cos\left[C_k \left(x - d/2 \right) \right] \tag{31}$$

The general solution of g_k is obtained with the same boundary condition as in the previous study except that equation (12) becomes:

$$\Delta n_0\left(x, z = W_e + W\right) = \frac{n_i^2}{\overline{N_a}} \times \left[\exp\left(\frac{V_j}{V_T} \right) - 1 \right] \tag{32}$$

So, g_k is expressed as follows:

$$g_k(z)=\frac{n_i^2}{N_a}\frac{e^{\beta(H-W_b-z)}\left[v_k ch\left(v_k(H-z)\right)+(\gamma-\beta)sh\left(v_k(H-z)\right)\right]}{v_k ch\left(v_k W_b\right)+(\gamma-\beta)sh\left(v_k W_b\right)}\times\left[\exp\left(\frac{V_j}{V_T}\right)-1\right] \quad (33)$$

The expression of the dark current density J_{b0} in the base region is obtained by the same expression in equation (19).

In the same way, the dark current density J_{e0} in the emitter region can be written as:

$$J_{e0}=\sum_{j=1}^{\infty}\frac{n_i^2}{N_d}\frac{8q\sin\left(C_j d/2\right)D_p}{dC_j L_j\left(C_j d+\sin(C_j d)\right)}\left[\frac{ch\left(\frac{W_e}{L_j}\right)+\frac{D_p}{L_j S_p}sh\left(\frac{W_e}{L_j}\right)}{sh\left(\frac{W_e}{L_j}\right)+\frac{D_p}{L_j S_p}ch\left(\frac{W_e}{L_j}\right)}\right]\times\left[\exp\left(\frac{V_j}{V_T}\right)-1\right] \quad (34)$$

The diffusion dark current density J_d is given by:

$$J_d=J_{b0}+J_{e0}=J_{sd}\times\left[\exp\left(\frac{V_j}{V_T}\right)-1\right] \quad (35)$$

The saturation recombination dark current density in the space charge layer can be obtained by [19]:

$$J_r=\frac{qWn_i}{\sqrt{\tau_p\tau_n}}\left[\exp\left(\frac{V_j}{2V_T}\right)-1\right]=J_{sr}\left[\exp\left(\frac{V_j}{2V_T}\right)-1\right] \quad (36)$$

2.4 Conversion efficiency

The I-V characteristic of the thin film polycrystalline solar cell can be obtained if we consider the equivalent circuit model represented in Figure 2.

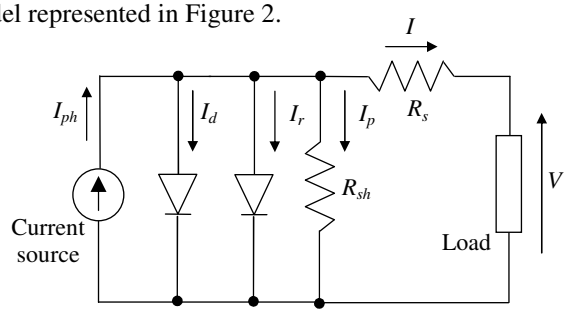

Fig. 2. A two-diode equivalent circuit for PV solar cell.

In this model, we consider the recombination both at the surface and at the bulk expressed by R_s and R_{sh} respectively. So, using Kirchhoff's first law, the current-voltage relationship I-V is expressed by:

$$I=I_{ph}-I_{sd}\left(\exp\left(\frac{V+R_s I}{V_T}\right)-1\right)-I_{sr}\left(\exp\left(\frac{V+R_s I}{2V_T}\right)-1\right)-\frac{V+R_s I}{R_{sh}} \quad (37)$$

where $I=A\times J$, (A=10^{-2} m^2).

The conversion efficiency of the cell is given by the formula:

$$Eff = \frac{I_m V_m}{A P_i} \tag{38}$$

4 Results and discussion

In this section, the results are obtained with the parameter values listed in Table 2. Using these parameters, we determine the conversion efficiency of the considered cell.

Table 2. Physical parameters of an elementary cell used in the computation results.

Parameters	Value
T (K)	300
ε_r	11,8
n_i (cm^{-3})	$1{,}45\times10^{10}$
R_{sh} ($\Omega.cm^2$)	500
K (J/K)	$1{,}3806\times10^{-23}$
ε_o ($F.cm^{-1}$)	$8{,}85\times10^{-14}$
R_s ($\Omega.cm^2$)	0,2
N_d (cm^{-3})	10^{18}
S_n (cm^2/s)	10^6
S_p (cm^2/s)	10^2
W_e (µm)	0,8
P_i (W/m^2)	925

Figure 3 demonstrates the variation of conversion efficiency according to the doping density N_{a2} in p-region of the cell at rear contact limit for d= 30 µm and $N_{a1}=7\times10^{15}cm^{-3}$. The study is developed for a different base thickness W_b (10µm, 20 and 50µm).

It can be seen that conversion efficiency increases with doping density N_{a2} and reaches maximum value. This result is associated to the Gaussian profile adopted in p-region that can be modulated by multi-junction that improves the open circuit voltage V_{oc}.

At high doping density N_{a2}, conversion efficiency decreases. This decrease is more important for a larger base thickness. In fact, the diffusion length decreases considerably when N_{a2} increases and consequently the short circuit current decreases. The values of doping density N_{a2} which correspond to the maximum conversion efficiency decrease when base thickness increases.

The optimum value of conversion efficiency can be obtained for a base thickness that is equal to the grain size and for $N_{a2} = 5\times10^{18}$ cm^{-3}. In this case, the conversion efficiency increase from 9,6% for $N_{a2}\approx N_{a1}$ to 13,75% for $N_{a2} = 5\times10^{18}$ cm^{-3}. Finally, it can be concluded that the Gaussian profile in base region considered in our model improves considerably the conversion efficiency and this improvement compared to standard n^+-p structure ($N_{a2}\approx N_{a1}$) is equal to 43%.

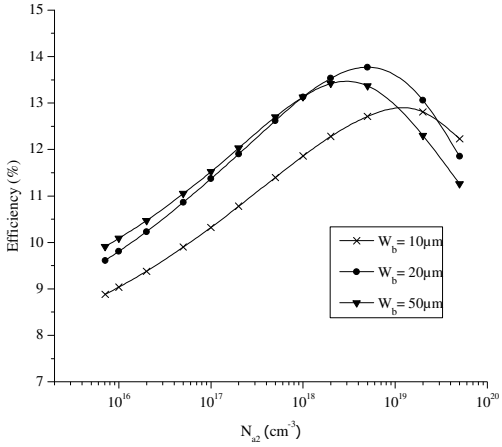

Fig. 3. Conversion efficiency as function of doping density at rear contact for different base thickness ($N_{a1}=7\times10^{15}cm^{-3}$, d=30µm, $V_g=10^6$cm/s).

With the same cell parameters, conversion efficiency is presented in Figure 4 as a function of doping density N_{a1} in p-region at the space charge limit for $N_{a2}= 5\times10^{18}$ cm^{-3}. We remark that conversion efficiency decreases when N_{a1} increases. This result is related to the decrease in the open circuit voltage of the cell which depends on the gradient concentration in p-region.

At high doping density N_{a1}, we remark a weak dependence of conversion efficiency on base thickness.

At low doping density, conversion efficiency varies with base thickness and the maximum value corresponds to W_b = 20µm. In fact, for this value, compromise between bulk generation and grain boundary recombination can be realized.

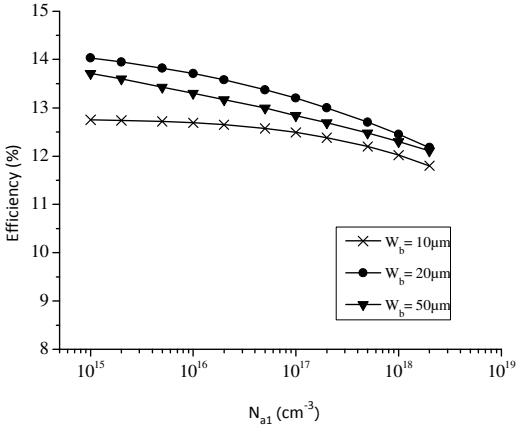

Fig. 4: Conversion efficiency as a function of doping density in p-region at space charge limit ($N_{a2}=5\times10^{18}cm^{-3}$, d=30µm, $V_g=10^6$cm/s).

Figure 5 shows the variation of conversion efficiency with respect to grain size d for $N_{a1}=7\times10^{15}cm^{-3}$ and $N_{a2}=5\times10^{18}cm^{-3}$.

We notice that conversion efficiency increases with grain size. Indeed, grain boundary recombination decreases then improves the collection of minority carrier at the n^+-p junction. At low grain width, conversion efficiency weakly depends on base thickness. In fact, grain boundary recombination is important and consequently base contribution in photocurrent becomes weak.

At large grain size, maximum conversion efficiency is obtained for large base thickness. This is due to the improved generation of minority carriers in the base region and the reduction of recombination at grain boundaries.

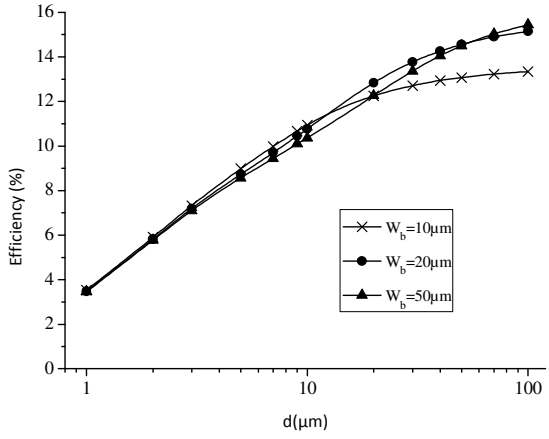

Fig. 5: Conversion efficiency as function of grain size ($N_{a2}=5\times10^{18}cm^{-3}$, $N_{a1}=7\times10^{15}cm^{-3}$, $V_g=10^6cm/s$)

5 Conclusion

In this paper, a 2-D model is applied to determine the conversion efficiency of n^+-p thin film polycrystalline solar cells by imposing a concentration gradient on base region. The influence of solar cell parameters such as base thickness, base doping profile and grain size on conversion efficiency is presented.

The results demonstrate that maximum conversion efficiency is obtained for a base thickness equal to grain dimension. In addition, the base doping profile considerably improves the open circuit voltage and the short circuit current, the optimum value of doping concentration at rear contact limit which corresponds to a maximum of conversion efficiency is equal to 5×10^{18} cm^{-3}.

Finally, we conclude that our proposed technique may be used to improve the conversion efficiency for a thin film polycrystalline solar cell.

References

1. S. A. Edmiston, G. Heiser, A. B. Sproul, M. A. Green, J. Appl. Phys. **80**, 12 (1996)
2. B. Ba, M. Kane, Solid-State Electron. **42**, 4 (1998)
3. A. Ben Arab, Solid-State Electron., **41**, 9 (1997)
4. A. Slaoui, E. Pihan, I. Ka, N.A. Mbow, S. Roques, J.M. Koebel, Sol. Energ. Mat. & Sol. Cells **90** (2006)
5. S. Martinuzzi, Solar Cells **12** (1984)
6. S. Narayanan, Wenham S. R., Green M.A. Appl. Phys. Lett. **48**, 13 (1986)
7. A. Kaminski, B. Vandelle, A. Fave, J.P. Boyeaux, Le Quan Nam, R. Monna, D. Sarti, A. Laugier, Sol. Energ. Mat. & Sol. cells **72**, 1-4 (2002)

8. J. Dugas, J. Oualid, Rev. Phys. Appl. **22**, 7 (1987)
9. J. Dugas, J.P. Crest, C.M. Signal, J. Oualid, Solid-State Electron. **26**, 11 (1983)
10. M. A. Green, Solid-State Electron. **21**, 9 (1978)
11. G. Mazetti, M. Severi, S. Solmi, IEEE Trans. On Electron. Dev. **30**, 7 (1983)
12. S. Swirhun, Y.H. Kwark , R.M. Swanson, IEDM techn. Dij. (1986)
13. S. N. Mohammed, C.E. Rogers, Solid-State Electron. **31**, 8 (1988)
14. S. N. Mohammed, M.A. Sobhan, S. Qutubuddin, Solid-State Electron. **32**, 10 (1989).
15. J. Dugas, Sol. Energ. Mat. & Sol. cells, **32**, 1 (1994)
16. J. Oualid, C.M. Signal, J. Dugas, J.P. Grest, H. Amzil, J. App. Phys. **55**, 4 (1984)
17. J. Del Alamo, S. Swirhun, R.M. Swanson, IEDM techn. Dij. (1985)
18. S. M. Sze, *In: Physics of semiconductor devices*, (New Jersey, Murry Hill: bell laboratories Inc. (1991)